EPJ Photovoltaics **5**, 55206 (2014)
www.epj-pv.org
DOI: 10.1051/epjpv/2014007

Substrate and p-layer effects on polymorphous silicon solar cells

S.N. Abolmasov[1,a], H. Woo[1], R. Planques[1], J. Holovský[2], E.V. Johnson[1], A. Purkrt[2], and P. Roca i Cabarrocas[1]

[1] LPICM, CNRS, École Polytechnique, 91128 Palaiseau, France
[2] Institute of Physics, ASCR v.v.i. Cukrovarnická, Prague, Czech Republic

Received: 30 July 2013 / Accepted: 11 June 2014
Published online: 16 July 2014

Abstract The influence of textured transparent conducting oxide (TCO) substrate and *p*-layer on the performance of single-junction hydrogenated polymorphous silicon (*pm*-Si:H) solar cells has been addressed. Comparative studies were performed using *p-i-n* devices with identical *i*/*n*-layers and back reflectors fabricated on textured Asahi U-type fluorine-doped SnO_2, low-pressure chemical vapor deposited (LPCVD) boron-doped ZnO and sputtered/etched aluminum-doped ZnO substrates. The *p*-layers were hydrogenated amorphous silicon carbon and microcrystalline silicon oxide. As expected, the type of TCO and *p*-layer both have a great influence on the initial conversion efficiency of the solar cells. However they have no effect on the defect density of the *pm*-Si:H absorber layer.

1 Introduction

General trends in thin film silicon (Si) photovoltaics are the reduction of the production costs and improvement of the conversion efficiency. The state of the art in thin film silicon solar cells utilizes tandem structures which pair a hydrogenated amorphous Si (*a*-Si:H) top cell with a hydrogenated microcrystalline Si (*μc*-Si:H) bottom cell. The efficiency and cost of these tandem cells are mainly limited by the light-induced degradation of *a*-Si:H and the low absorption coefficient/deposition rate of *μc*-Si:H, respectively [1]. Therefore, there has been considerable interest recently in wide band gap nanostructured Si materials which may offer better performance/stability to the top cell and allow reducing the thickness of the bottom cell using enhanced light trapping techniques. These nanostructured Si materials mainly include hydrogenated amorphous and microcrystalline silicon oxide (*a*- and *μc*-SiO:H) [2–8], protocrystalline (*pc*-Si:H) [9] and polymorphous (*pm*-Si:H) silicon [10] that could be used as alternatives to standard doped and absorber layers, respectively. On the other hand, the light trapping is mainly realized by texturing of transparent conductive oxide (TCO) layers on glass substrates [11]. However, this approach tends to deteriorate the electrical parameters of the cells with both *a*- and *μc*-Si:H absorber layers [12,13]. The goal of this study is to evaluate the performance of single-junction (*p-i-n*) *pm*-Si:H solar cells on different textured TCO substrates which also incorporate *p*-type silicon oxide films as the window layer. To examine the substrate and *p*-layer effects on *pm*-Si:H solar cell performance, the cells were fabricated with the same *i*- and *n*-layers.

2 Experimental

Silicon films were deposited in a 13.56 MHz radio-frequency plasma enhanced chemical vapor deposition (RF-PECVD) system, consisting of a single vacuum vessel containing three independent plasma chambers [14]. Mixtures of $H_2/SiH_4/CO_2/B(CH_3)_3$, H_2/SiH_4 and $H_2/SiH_4/PH_3$ were used as source gases for the growth of *p*-type *a*-SiO:H, intrinsic *pm*-Si:H and *n*-type *a*-Si:H or *μc*-Si:H, respectively. The *p-i-n* devices were fabricated on textured Asahi U-type fluorine-doped tin oxide (SnO_2:F), low-pressure chemical vapor deposited (LPCVD) boron-doped (ZnO:B) ZnO (type A), and RF sputtered and etched (sp-e) aluminum-doped zinc oxide (ZnO:Al) coated glass substrates (1 mm thick). Details on TCO deposition processes along with TCO characteristics can be found in references [15–17]. Aluminum back contacts were deposited by thermal evaporation. Sputtered ZnO/Ag stacks were also used as back reflectors to enhance the light trapping from the back side of the device. The cells areas were defined by using a shadow mask (0.126 cm^2). Fourier transform photocurrent spectroscopy (FTPS) [18] was used to determine the effect of the TCO substrate on the absorption coefficient (α) and defect density of *pm*-Si:H in the cells. Dark conductivity (σ_d) of *p*-type silicon oxide on Corning 7059 glass was measured using a coplanar Al electrode configuration. The optical properties and thickness of the films were measured

[a] e-mail: sergey.abolmasov@polytechnique.edu

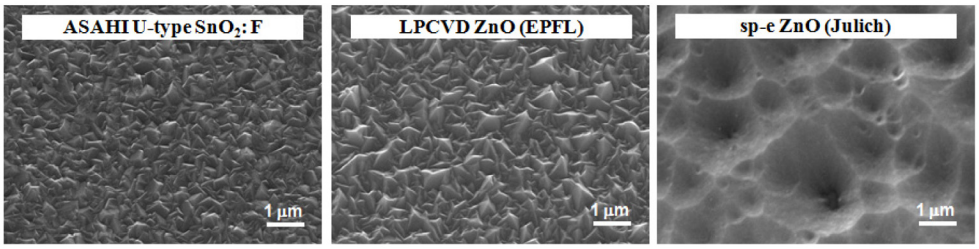

Fig. 1. Scanning electron microscope (SEM) images of textured TCO substrates used in this study (top view under an angle of 30°).

with UV-visible spectroscopic ellipsometry (SE). The *J*-*V*-characteristics and external quantum efficiency (EQE) of the solar cells were measured under 1 sun illumination at 25 °C. A 1-mm-diameter orifice was used for the EQE and reflectivity measurements. Most results were obtained on cells in the annealed state (40 min at 150 °C). Accelerated light-induced degradation (LID) tests were performed at approximately 2 suns in a home-made LID system using Oriel Apex illuminator (Model 71223) with a quartz tungsten halogen lamp. The cell temperature was kept at 50 °C. In this case, the *J*-*V*-characteristics were measured in situ using the same lamp and a neutral density filter, resulting in a light exposure equivalent to 1 sun.

3 Results and discussion

The surface morphologies of the textured TCO substrates used in this study are shown in Figure 1. It is obvious that the front TCO layer has to exhibit high transparency in the useful spectrum range and a sufficient conductivity to limit the series resistance of the cell. However, it must also have sufficient surface roughness to optimize the light confinement [11]. It can be seen in Figure 1 that there is a significant difference in the surface roughness of the three TCO layers. Both SnO_2 and LPCVD ZnO have pyramidal features with sizes below 500 nm that are well suited for effective light trapping in *a*-Si:H solar cells. On the other hand, sp-e ZnO has much smoother surface with lateral features that are more than 1 μm in size and therefore is more suited for the use in μc-Si:H solar cells. Because the properties of TCO may also vary significantly, appropriate window *p*-layers should be developed. For example, it is well known that a textured SnO_2 front contact is susceptible to reduction by hydrogen [19, 20]. Therefore, ZnO has recently been investigated as an alternative that is both resistant to hydrogen plasma induced darkening and has higher transmission. However, fabrication of *p*-*i*-*n* devices on ZnO results in a lower fill factor (*FF*), which is believed to be due to a rectifying contact that is formed between the *p*-type *a*-Si:H and the *n*-type ZnO layer [21]. There have been numerous attempts to overcome this problem [22–25], but there is still lack of a complete understanding of the phenomenon. The most efficient way to overcome the problem is to use an ultrathin μc-Si:H or silicon oxide (μc-SiO:H) *p*-layer, which is more conducting than a hydrogenated amorphous silicon carbide (*a*-SiC:H) *p*-layer [2, 4, 5].

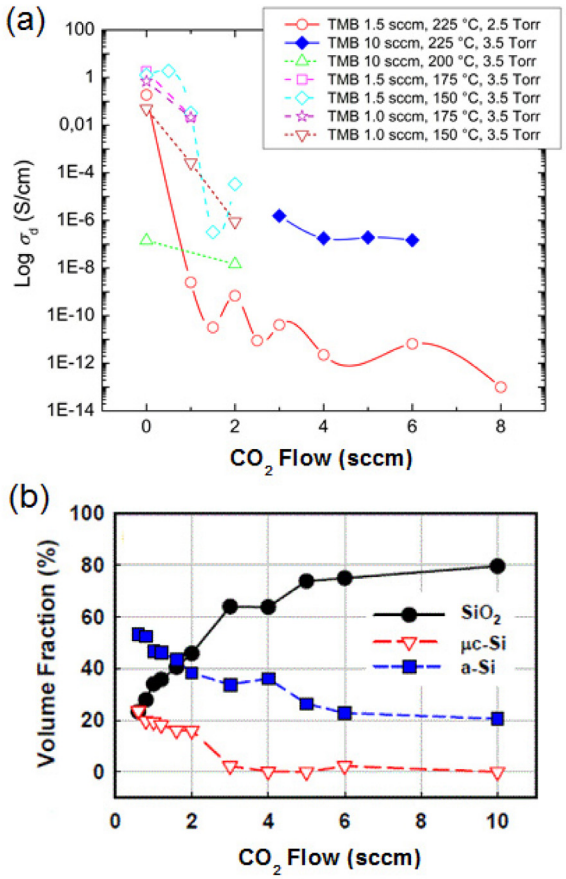

Fig. 2. (a) Dark conductivity (at room temperature) of *p*-type silicon oxide thin films as a function of CO_2 flow rate (the films were grown on Corning glass at H_2 (500 sccm)/SiH_4 (10 sccm) =50 and with 2% $B(CH_3)_3$ in H_2) and (b) evolution of SiO_2, *a*-Si and μc-Si volume fractions of optimized μc-SiO:H *p*-layer with increasing CO_2 flow rate, as deduced from the BEMA modeling.

Like the TCO layer, the window layer should also exhibit high transparency and sufficient conductivity. For the silicon oxide *p*-layer deposition, a wide range of deposition parameters such as RF power, inter-electrode distance, substrate temperature, gas composition, pressure and flow were optimized. It turns out that lowering the CO_2 and $B(CH_3)_3$ concentration favors the growth of conductive silicon oxide *p*-layers, as shown in Figure 2a. The results of SE measurements/modeling for optimized *p*-layers grown at p = 3.5 Torr, T = 175 °C and a TMB

Table 1. Initial photovoltaic parameters of *pm*-Si:H *p*-*i*-*n* devices fabricated on three different TCO substrates along with the absorption coefficient and the Urbach energy of their intrinsic *pm*-Si:H layer. All the cells incorporate the same *i*-*pm*-Si:H (300 nm) and *n*-*a*-Si:H layers and evaporated Al back contacts.

Sample #	TCO/*p*-layer description	α (1.2 eV) (cm^{-1})	E_U (meV)	FF (%)	V_{OC} (V)	J_{SC} (mA/cm^2)	Eff. (%)
1207271	ASAHI SnO_2 (ref) *a*-SiC *p*-layer	0.15 ± 0.03	39.9 ± 2	71.77	0.868	12.65	7.88
1208071I	LPCVD ZnO μc-SiO_x *p*-layer #1	0.18 ± 0.02	39.6 ± 0.8	69.71	0.853	11.19	6.65
1208071J	sp-e ZnO μc-SiO_x *p*-layer #1	0.13 ± 0.05	37.8 ± 1.5	66.23	0.881	10.08	5.88

Table 2. Initial photovoltaic parameters of *pm*-Si:H *p*-*i*-*n* devices fabricated on three different TCO substrates. All the cells incorporate the same *p*-μc-SiO:H, *i*-*pm*-Si:H (250 nm) and *n*-μc-Si:H layers and sputtered ZnO-Ag back contacts.

Sample #	TCO/*p*-layer description	FF (%)	V_{OC} (V)	J_{SC} (mA/cm^2)	Eff. (%)
1301245I	LPCVD ZnO μc-SiO_x *p*-layer #2	68.54	0.903	14.83	9.2
1301245J	sp-e ZnO μc-SiO_x *p*-layer #2	61.09	0.918	13.54	7.6
1301245A	ASAHI SnO_2 μc-SiO_x *p*-layer #2	55.27	0.793	13.69	6.0

flow rate of 1.5 sccm indicate that the optical band-gap energy (E_g) of these thin films can be increased from 1.95 to 2.8 eV by increasing the CO_2 flow rate from 1 to 10 sccm. The increase in E_g is mainly due to an increase in the oxygen concentration, whereas the conductivity of these films is controlled by their μc-Si fraction as determined from the modeling of the spectroscopic ellipsometry data. The measured spectra were modeled using the Bruggeman's effective medium approximation (BEMA) [26], in which the silicon oxide material was considered as being a physical combination of three distinct phases formed by SiO_2, *a*-Si and μc-Si. Figure 2b shows that the μc-Si fraction in our optimized silicon oxide *p*-layer, according to the BEMA model, does not exceed 20% and sharply decreases with increasing the CO_2 mass flow rate above 2 sccm [27]. In our case the silicon oxide *p*-layer was grown at a CO_2 mass flow rate of 1 sccm. Such a layer has a 19% μc-Si fraction and thereby referred to as μc-SiO:H in the paper.

In the first series of experiments, the TCO/*p*-layer and *p*/*i* interface regions of the cells deposited on the three types of TCO substrates were systematically improved by introducing thin buffer layers. By optimizing the doping profile (by adding one or more layers grown with different gas composition) and thickness of the window *p*-layer, the cell current was improved while maintaining relatively high FF and open circuit voltage (V_{OC}). Typically the *p*-layer was a 3-layer-stack consisting of an ultra-thin μc-Si:H, a heavily doped μc-SiO:H and a lightly doped μc-SiO:H layer. Such multilayer structure provides a wider process window, enabling the use of much thinner window *p*-layer. Consequently, short-circuit current J_{SC} and V_{OC} were enhanced with only a small drop in FF. Since the growth of both μc-SiO:H and *pm*-Si:H requires a hydrogen rich plasma, an *a*-SiC:H *p*-layer was used in the case of SnO_2 substrate and served as a reference. Moreover, FTPS was used to check the quality of the *pm*-Si:H in the cells grown on the three TCO substrates. Interestingly enough, the FTPS results, obtained for the cells with a 300 nm thick intrinsic layer and an *a*-Si:H *n*-layer, shown in Figure 3 indicate very similar *pm*-Si:H material properties in the cells with a defect density below 5×10^{15} cm^{-3} and Urbach energy about 40 meV. This contrasts with quite different values for the solar cell parameters summarized in Table 1, which did show a strong dependence on the TCO and *p*-layer type, thus suggesting that the surface roughness as well as the TCO/*p*-layer and *p*/*i* interface regions play very important roles in determining the overall cell performance. Similar results have been reported for μc-Si:H *p*-*i*-*n* devices and it was also demonstrated that the FTPS method is sensitive to bulk material properties but not to local shunts induced by TCO morphology [28].

Further optimization of the μc-SiO:H *p*-layer/*i* interface and introduction of ZnO/Ag back contacts along with a μc-Si:H *n*-layer, however, resulted in great enhancement of J_{SC} and V_{OC} in the cells on ZnO substrates, as can be seen in Table 2. Among the three different TCO substrates, sp-e ZnO showed the highest $V_{OC} \sim 0.92$ V, whereas LPCVD ZnO led to the highest $J_{SC} \sim 14.8$ mA/cm^2 for the same *p*-*i*-*n*/metal contact configuration. These two facts could be related directly to the TCO surface morphology: a smooth surface has smaller number of defects than a rough one, simply because of the difference in the surface area, resulting in higher V_{OC}. On the contrary, a rough surface results in light scattering and, in turn, in better light trapping. The use of the same μc-SiO:H *p*-layer on SnO_2 substrates, however, resulted in a deterioration of all solar cell parameters due to hydrogen plasma induced reduction of SnO_2, as mentioned above. Figure 4 shows a comparison

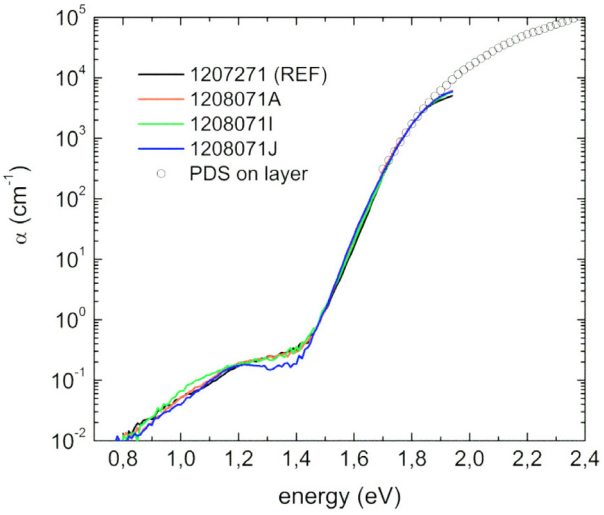

Fig. 3. Absorption coefficient of *pm*-Si:H absorber layer in *p*-*i*-*n* devices fabricated on Asahi SnO_2, LPCVD ZnO and sp-e ZnO substrates versus photon energy measured by FTPS. The absolute scaling is made relative to *i*-layer on Corning glass measured by photothermal deflection spectroscopy (PDS).

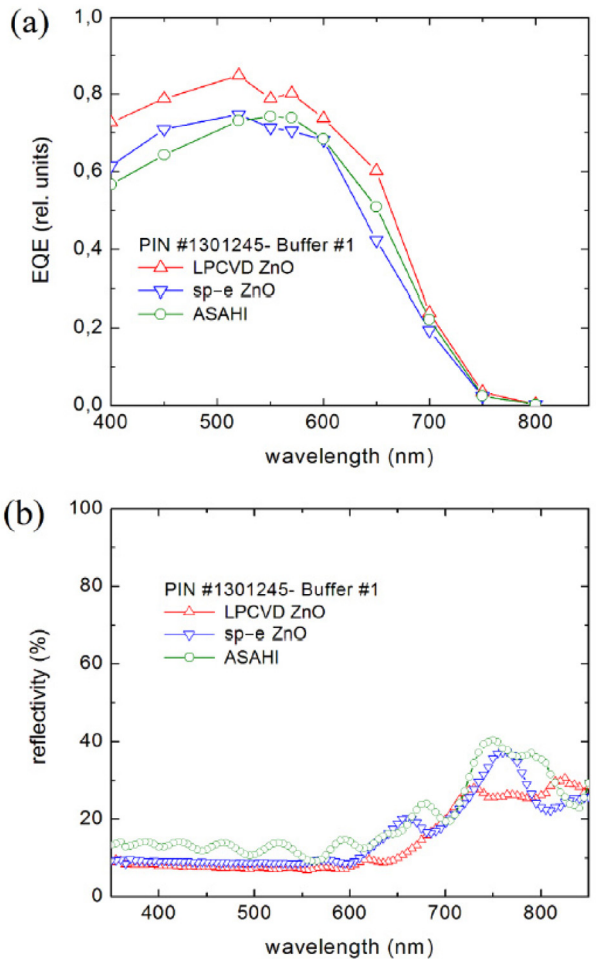

Fig. 4. External quantum efficiency of *pm*-Si:H solar cells with the same *p*-*i*-*n*/metal contact configuration fabricated on three different TCO substrates. A thin *a*-Si:H buffer layer is used at the *p*/*i* interface. The cells are measured in their initial state. Photovoltaic parameters of these devices are summarized in Table 2.

of EQE and reflectivity curves of the three *p*-*i*-*n* devices with a 250 nm thick *pm*-Si:H layer, indicating excellent spectral response in the blue part of the spectrum for the *p*-*i*-*n* device on LPCVD ZnO, thanks to our newly developed μc-SiO:H *p*-layer. One can see (Fig. 4b) that the *p*-*i*-*n* on SnO_2 has higher reflectivity due to SnO_2 reduction by hydrogen, as mentioned above. Note that the highest J_{SC} value for LPCVD ZnO was also confirmed independently by EQE measurements at EPFL and PTB. Nevertheless, this value is still below that (16.75 mA/cm^2) obtained in the champion *p*-*i*-*n* device with an a-Si:H absorber layer of the same thickness (250 nm) and Oerlikon LPCVD ZnO (front and back contact) [29]. This is partly due to the fact that *pm*-Si:H has larger optical band gap and lower optical absorption compared to *a*-Si:H. For example, E_{04}, defined as the energy at which the absorption coefficient is equal to 10^4 cm^{-1}, lies approximately in the range between 1.7–1.8 eV and 1.8–1.9 eV [27,30] (see also Fig. 3) for *a*-Si:H and *pm*-Si:H, respectively. It should also be mentioned that the champion a-Si:H solar cell has an anti-reflection coating and a LPCVD ZnO/white paint back contact.

Last but not least, it has been shown recently that the regions around the window *p*-layer could also have an influence on the stability of single-junction *pm*-Si:H solar cells. In particular, localized delamination of the TCO/*p*-layer interface in *pm*-Si:H solar cells fabricated on textured SnO_2 substrates was observed during the initial stage of light-soaking [31]. Note that *pm*-Si:H was produced in a hydrogen rich plasma and hence contains more hydrogen than standard *a*-Si:H. It was proposed in reference [31] that the light-soaking of *pm*-Si:H introduces structural changes related to the diffusion of molecular hydrogen in the material with subsequent accumulation at the TCO/*p*-layer interface which finally causes localized delamination of the interface, affecting the solar cell parameters in an irreversible way (no recovery with thermal annealing). It is reasonable therefore to assume that the use of different TCO and/or *p*-layers may affect localized delamination of the interface. Note, however, that in reference [31] a xenon lamp was used to perform the light-soaking. To examine the effect further we used a home-made LID system in which a halogen lamp was employed instead of Xe lamp. Using this LID system it was found that the type of TCO and TCO/*p*-layer interface have no effect on the initial light-induced degradation dynamics of *pm*-Si:H solar cells and no irreversible behavior was observed in our solar cells. This discrepancy is most likely due to fact that the two lamps mentioned above have very different spectral compositions: quartz tungsten halogen lamps have the spectrum with a broad maximum around 800 nm and a sharp decrease between 500 and 350 nm, whereas Oriel Apex Xe lamps have an almost flat maximum in the range 350–800 nm [32]. Note that the maximum of solar radiation spectrum (AM1.5) lies in the

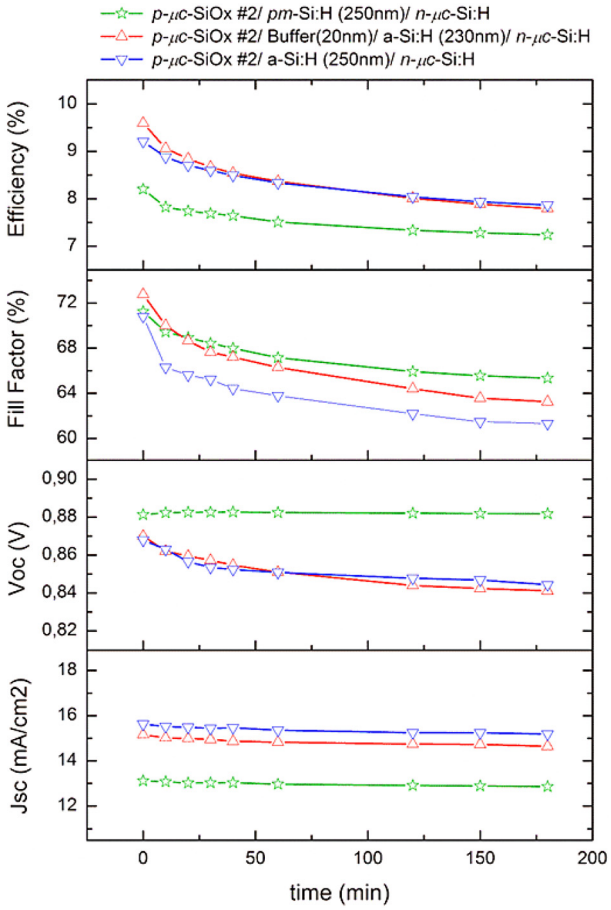

Fig. 5. Evolution of photovoltaic parameters of three different p-i-n solar cells during the light-soaking under a halogen lamp illumination at 2 suns. All three cells are fabricated on LPCVD ZnO using sputtered ZnO-Ag back contacts; their p-i-n structures are shown at the top of graph. Note that the J-V-characteristics are measured using the same halogen lamp at 1 sun and 50 °C.

range of 500–600 nm. Taking into account the fact that SnO_2 substrates are quite transparent to the blue light it is likely that a long exposure of p-i-n devices on their basis using a Xe lamp can result in severe damage of the region near the p/i interface.

Because the state-of-the-art tandem silicon solar cells incorporate a-Si:H top cells it is interesting to make a direct comparison of the LID dynamics in a-Si:H and pm-Si:H cells with the same thickness of intrinsic layers. Figure 5 shows such a comparison including an a-Si:H solar cell with a thin (20 nm) pm-Si:H buffer layer. It is seen that degradation of J_{SC} is negligibly small for the three cells with the initial J_{SC} values controlled by i-layer band gap while most of degradation is caused by a substantial decrease in FF – a common drawback among a-Si:H p-i-n devices [33,34]. The decrease in FF is however more severe for a-Si:H cell than for pm-Si:H cell. Even though the insertion of a thin pm-Si:H buffer layer can improve the initial FF and conversion efficiency of a-Si:H cell, it has no effect on the conversion efficiency after 1 h of light-soaking: the efficiency of a-Si:H cell with a pm-Si:H buffer layer becomes equal to that of pure a-Si:H cell. Still the pm-Si:H cell is the one which maintains the highest FF value on the long run, as recently reported for light-soaking times up to 1000 h [35]. Another distinguished feature of solar cells with absorber layers grown at high hydrogen dilution is that V_{OC} of these cells usually increases with light-soaking time [31,36], as can be seen in Figure 5 for pm-Si:H p-i-n device. However, despite of their better stability the efficiency of pm-Si:H solar cells is mainly limited by lower optical absorption, as shown above. Thus, realization of effective light-trapping in single-junction pm-Si:H solar cells on textured TCO substrates is a challenging task and so far LPCVD ZnO shows the highest J_{SC}. Nevertheless, higher values of stabilized FF and V_{OC} for pm-Si:H material make it attractive for the use in multi-junction devices, e.g. in triple junction solar cells that do not require high J_{SC}.

4 Conclusions

The effects of textured TCO substrate and p-layer on the performance of single-junction (p-i-n) pm-Si:H solar cells have been evaluated. It turns out that the type of TCO and p-layer both have a great influence on the initial conversion efficiency of the solar cells. A μc-SiO:H p-layer was successfully implemented in the cells based on ZnO substrates, resulting in great enhancement of their performance. In particular, the cells grown on LPCVD ZnO had the highest J_{SC} and initial η, whereas those on sp-e ZnO had the highest V_{OC}. Unlike the strong influence on the initial efficiency, the TCO type and TCO/p-layer interface had no effect on the defect density of pm-Si:H absorber layer. The obtained results allow to conclude that pm-Si:H is more suitable for the use in multi-junction devices such as in 3J solar cells rather than in single-junction devices, mainly due to its improved stability compared to a-Si:H.

This work was carried out in the framework of the FP7 project “Fast Track”, funded by the EC under grant agreement No. 283501. The authors thank the Forschungszentrum Jülich and IMT’s PV-lab (EPFL) for preparation of textured ZnO substrates. The help of Dr. Ingo Kröger (PTB, Brunswick) and Dr. Martin Foldyna (LPICM) in validation of EQE measurements is also gratefully acknowledged.

References

1. C.A. Wolden et al., J. Vac. Sci. Technol. A **29**, 030801 (2010)
2. K. Schwanitz, S. Klein, T. Stolley, M. Rohde, D. Severin, R. Trassl, Sol. Energy Mater. Sol. Cells **105**, 187 (2012)
3. A. Lambertz, F. Finger, B. Hollaender, J.K. Rath, R.E.I. Schropp, J. Non-Cryst. Solids **358**, 1962 (2012)
4. S. Inthisang, T. Krajangsang, I.A. Yunaz, A. Yamada, M. Konagai, C.R. Wronski, Phys. Stat. Sol. C **8**, 2990 (2011)

5. P. Cuony, M. Marending, D.T.L. Alexander, M. Boccard, G. Bugnon, M. Despeisse, C. Ballif, Appl. Phys. Lett. **97**, 213502 (2010)
6. A. Sarker, A.K. Barua, Jpn J. Appl. Phys. **41**, 765 (2002)
7. P. Sichanurgist, T. Yoshida, Y. Ichikawa, H. Sakai, J. Non-Cryst. Solids **164–166**, 1081 (1993)
8. H. Watanabe, K. Haga, T. Lohner, J. Non-Cryst. Solids **164–166**, 1085 (1993)
9. C.R. Wronski, J.M. Pearce, R.J. Koval, A.S. Ferlauto, R.W. Collins, in *World Climate and Energy Event Proceedings*, *Rio de Janeiro, Brazil, 2002*, p. 67
10. P. Roca i Cabarrocas, Y. Djeridane, Th. Nguyen-Tran, E.V. Johnson, A. Abramov, Q. Zhang, Plasma Phys. Control. Fusion **50**, 124037 (2008)
11. M. Boccard et al., IEEE J. Photovolt. **2**, 229 (2012)
12. M. Despeisse, G. Bugnon, A. Feltrin, M. Stueckelberger, P. Cuony, F. Meillaud, A. Billet, C. Ballif, Appl. Phys. Lett. **96**, 73507 (2010)
13. M. Python, O. Madani, D. Dominé, F. Meillaud, E. Vallat-Sauvain, C. Ballif, Sol. Energy Mater. Sol. Cells **93**, 1714 (2009)
14. P. Roca i Cabarrocas, J.B. Chevrier, J. Huc, A. Lloret, J.Y. Parey, J.P.M. Schmitt, J. Vac. Sci. Technol. A **9**, 2331 (1991)
15. K. Sato, Y. Gotoh, Y. Wakayama, Y. Hayashi, K. Adachi, H. Nishimura, Reports Res. Lab. Asahi Glass Co. Ltd. **42**, 129 (1999)
16. S. Faÿ, J. Steihauser, N. Oliveira, E. Vallat-Sauvain, C. Ballif, Thin Solid Films **515**, 8558 (2007)
17. J. Müller, B. Rech, J. Springer, M. Vanecek, Sol. Energy **77**, 917 (2004)
18. J. Holovsky, in *Fourier Transforms – New Analytical Approaches and FTIR Strategies*, edited by G. Nikolic (InTech, 2011), p. 257
19. H. Schade, Z.E. Smith, J.H. Thomas, A. Catalano, Thin Solid Films **117**, 149 (1984)
20. S. Kumar, B. Drevillon, J. Appl. Phys. **65**, 3023 (1989)
21. E. Bohmer, F. Siebke, B. Rech, C. Beneking, H. Wagner, Mater. Res. Soc. Symp. Proc. **420**, 519 (1996)
22. M. Kubon, E. Boehmer, F. Siebke, B. Rech, C. Beneking, H. Wagner, Sol. Energy Mater. Sol. Cells **14–42**, 485 (1996)
23. K. Minegishi, Y. Koiwai, Y. Kikuchi, K. Yano, M. Kasuga, A. Shimizu, Jpn J. Appl. Phys. Part 2 **36**, L1453 (1997)
24. G. Ganguly, D.E. Carlson, S.S. Hegedus, D. Ryan, R.G. Gordon, D. Pang, R.C. Reedy, Appl. Phys. Lett. **85**, 479 (2004)
25. S. Baek, J.C. Lee, Y.J. Lee, S.M. Iftiquar, Y. Kim, J. Park, J. Yi, Nanoscale Res. Lett. **7**, 81 (2012)
26. G.E. Gellison, in *Ellipsometry Handbook*, edited by H.G. Tompkins, E.A. Irene (William Andrew, Highland Mills, 2005)
27. K.H. Kim, Ph.D. thesis, École Polytechnique, 2012
28. G. Bugnon, G. Parascandolo, T. Söderström, P. Cuony, M. Despeisse, S. Hänni, J. Holovský, F. Meillaud, C. Ballif, Adv. Funct. Mater. **22**, 3665 (2012)
29. S. Benagli, D. Borrello, E. Vallat-Sauvain, J. Meier, U. Kroll, J. Hötzel, J. Spitznagel, J. Steinhauser, L. Marmello, G. Monteduro, L. Castens, in *Proceedings of the 24th European Photovoltaic Solar Energy Conference, Hamburg, Germany, 2009*, p. 2293
30. P. Roca i Cabarrocas, A. Fontcuberta i Morral, Y. Poissant, Thin Solid Films **403-404**, 39 (2002)
31. K.H. Kim, E.V. Johnson, P. Roca i Cabarrocas, Sol. Energy Mater. Sol. Cells **105**, 208 (2012)
32. Newport Spectral Irradiance Data, www.newport.com
33. H. Sakai, T. Yoshida, S. Fujikake, T. Hama, Y. Ichikawa, J. Appl. Phys. **67**, 3494 (1990)
34. A. Kolodziej, Opto-Electron. Rev. **12**, 21 (2004)
35. K.H. Kim, S. Kasouit, E.V. Johnson, P. Roca i Cabarrocas, Sol. Energy Mater. Sol. Cells **119**, 124 (2013)
36. P. Siamchai, M. Konagai, Appl. Phys. Lett. **67**, 3468 (1995)

Cite this article as: S.N. Abolmasov, H. Woo, R. Planques, J. Holovský, E.V. Johnson, A. Purkrt, P. Roca i Cabarrocas, Substrate and p-layer effects on polymorphous silicon solar cells, EPJ Photovoltaics **5**, 55206 (2014).